Intramolecular 1,*n* Palladium Migrations in Polycyclic Aromatic Hydrocarbons. Palladium(II) versus Palladium(IV) Mechanisms: A Theoretical Study

Antonio J. Mota† and Alain Dedieu*

Laboratoire de Chimie Quantique, Institut de Chimie, LC3-UMR 7177 CNRS/ULP, Université Louis Pasteur, Strasbourg, 4 Rue Blaise Pascal, 67000 Strasbourg, France

Received February 10, 2006

DFT/B3LYP calculations have been carried out to study intramolecular 1,*n* aryl-to-aryl palladium shifts ($n = 3-6$) in polyaryl systems. Such rearrangements, which are associated with a concomitant shift of a hydrogen atom, have been found experimentally to be a pivotal step of several organic transformations mediated by palladium complexes. From the calculations of the various transition states and intermediates involved in the process, the intimate mechanism for the 1,3 shift is shown to correspond to a Pd(IV) pathway, whereas a Pd(II) pathway is favored in the case of 1,5 and 1,6 migrations. In the case of 1,4 migrations, both mechanisms become competitive. The Pd(IV) pathway can involve either a true Pd(IV) intermediate (oxidative addition mechanism) or a Pd(IV) transition state (oxidative hydrogen migration mechanism). The energy barrier is very high for the 1,3 palladium shift, making this process very unlikely, in contrast to the other ones, which have enthalpy barriers ranging between 17.8 and 27.5 kcal mol^{-1}.

Introduction

Multistep organic transformation reactions mediated or catalyzed by palladium complexes are extraordinary numerous and diversified.[1,2] They encompass a large variety of elementary steps that very often involve a reversible interconversion between two oxidation states, generally 0 and +2. The interconversion between the +2 and +4 oxidation state is more controversial, since there are still only very few examples of characterized Pd(IV) complexes, especially with palladium−carbon bonds.[3−7] Thus the recent observation of 1,4 and 1,5 palladium migration, associated with a concomitant shift of the hydrogen, between two carbon atoms (either sp^2 as in Scheme 1 or sp^3)[8−14] is quite intriguing from the mechanistic point of view.

Scheme 1. General Pathways for the Aryl-to-Aryl Pd Shift

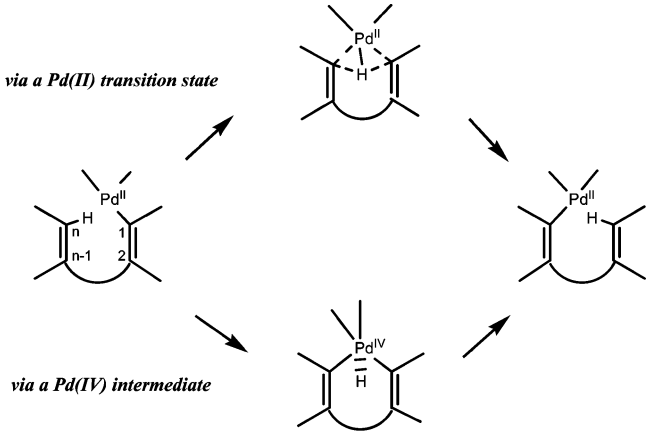

As shown in Scheme 1, for an overall aryl-to-aryl shift two different intramolecular pathways may be envisioned: either (i) a two-step process that goes via a C−H oxidative addition on the palladium atom to yield a hydridopalladium(IV) intermediate, which subsequently undergoes a C−H reductive elimination toward a neighboring carbon atom,[15] or (ii) a one-step process in which the oxidation state +2 of the palladium atom is retained. In this case it could be considered either as a metathesis reaction of the C−H σ bond with the Pd−C bond or as a concomitant 1,*n* shift of both the hydrogen and the palladium atoms. The experimental studies that have been carried out so far have shown the importance of this process from a synthetic point of view, since it allows the attachment

* To whom correspondence should be addressed. E-mail: dedieu@quantix.u-strasbg.fr. Tel: +33-3-90-241305. Fax: +33-3-90-241589.

† Present address: Departamento de Química Inorgánica, Universidad de Granada, Campus de Fuentenueva, 18071-Granada, Spain.

(1) For some recent references see: (a) Tsuji, J. *Palladium Reagents and Catalysis: New Perspectives for the 21st Century*; John Wiley & Sons: New York, 2004. (b) *Handbook of Organopalladium Chemistry for Organic Synthesis*; Negishi, E., Ed.; John Wiley & Sons: New York, 2002. (c) See also chapters 5, 6, 8−10, 13, and 15 in: *Metal-Catalyzed Cross-Coupling Reactions*, 2002 ed; de Meijere A., Diederich, F., Eds.; Wiley-VCH: Weinheim, Germany, 2004; Chapter 5, pp 2217−2317.

(2) See also: (a) Negishi, E.; Copéret, C.; Ma, S.; Liou, S.-Y.; Liu, F. *Chem. Rev.* **1996**, 1365. (b) Herrmann, W. A.; Öfele, K.; Preysing, D. v.; Schneider, S. K. *J. Organomet. Chem.* **2003**, *687*, 1229. (c) Palladium Chemistry in 2003: Recent Developments, special issue (Volume 687) of *J. Organomet. Chem.*; Bertrand, G., Ed. (d) Zeni, G.; Larock, R. C. *Chem. Rev.* **2004**, *104*, 2285. (e) Tietze, L. F.; Ila, H.; Bell, H. P. *Chem. Rev.* **2004**, *104*, 3453. Dupont, J.; Consort, C. S.; Spencer, J. *Chem. Rev.* **2005**, *105*, 2527.

(3) Canty, A. J. *Acc. Chem. Res.* **1992**, *25*, 83.

(4) Canty, A. J.; van Koten, G. *Acc. Chem. Res.* **1995**, *28*, 406.

(5) Canty, A. J. In *Handbook of Organopalladium Chemistry for Organic Synthesis*; Negishi, E. I., Ed.; Wiley: New York, 2002; Vol. 1, Chapter II.4, p 189.

(6) Catellani, M. *Synlett* **2003**, 298.

(7) van Belzen, R.; Elsevier, C. J.; Dedieu, A.; Veldman, N.; Spek, A. L. *Organometallics* **2003**, *22*, 722.

(8) Wang, L.; Pan, Y.; Jiang, X.; Hu, H. *Tetrahedron Lett.* **2000**, *41*, 725.

(9) Karig, G.; Moon, M.-T.; Thasana, N.; Gallagher, T. *Org. Lett.* **2002**, *4*, 3115.

(10) Campo, M. A.; Larock, R. C. *J. Am. Chem. Soc.* **2002**, *124*, 14326.

(11) Campo, M. A.; Huang, Q.; Yao, T.; Tian, Q.; Larock, R. C. *J. Am. Chem. Soc.* **2003**, *125*, 11506.

(12) Huang, Q.; Fazio, A.; Dai, G.; Campo, M. A.; Larock, R. C. *J. Am. Chem. Soc.* **2004**, *126*, 7460.

(13) Zhao, J.; Larock, R. C. *Org. Lett.* **2005**, *7*, 701.

(14) Bour, C.; Suffert, J. *Org. Lett.* **2005**, *7*, 653.

10.1021/om060128a CCC: $33.50
Publication on Web 05/17/2006

Scheme 2. The Systems Studied for the 1,*n* Pd Migration

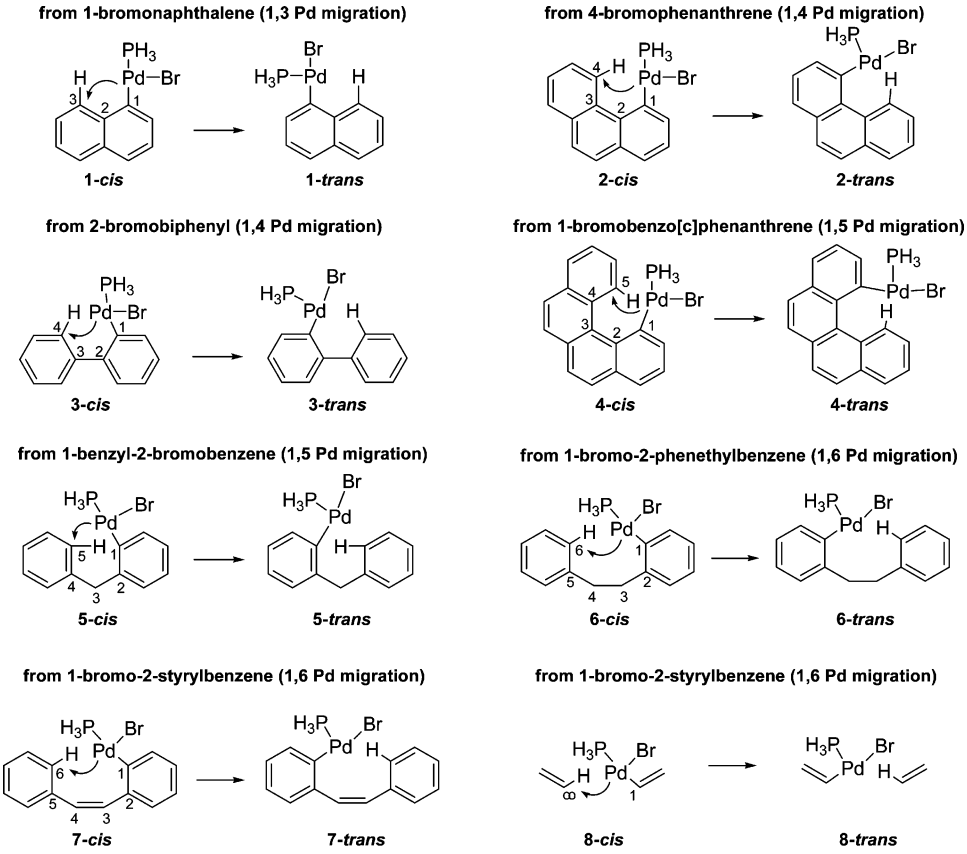

of groups in positions that are otherwise difficult to substitute by usual chemistry. However, they could not assess unambiguously which of these two pathways is operative. We have recently addressed this issue, via DFT-B3LYP calculations, for a 1,5 vinyl-to-aryl shift that took place in the course of a cyclocarbopalladation−Stille coupling tandem reaction.[16] In this case the intimate mechanism was found to correspond to a one-step proton transfer between the two negatively charged carbon atoms of the vinyl and the phenyl groups that are bound to the palladium atom in the transition state, thus retaining the +2 oxidation state of the palladium atom. That this transfer was relatively easy could be accounted for by relating it, through isolobal analogy arguments, to the hydrogen scrambling process in CH_5^+. We have now broadened the scope of our investigation and wish to report here our results for 1,3 to 1,6 aryl-to-aryl palladium migration.

Computational Details

The calculations were carried out at the DFT-B3LYP level[17−19] with the Gaussian 03 program.[20] The triphenylphosphine ligand

Scheme 3. Initial Oxidative Addition Process

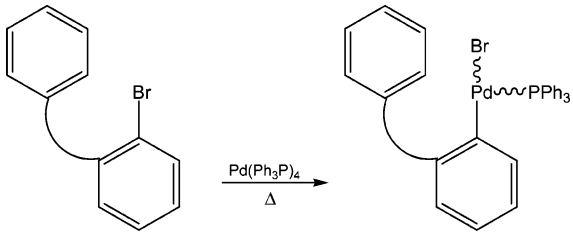

PPh_3 was modeled by PH_3. The geometries were fully optimized by the gradient technique with the following basis: For Pd the LANL2DZ basis set is modified following the prescription of Couty and Hall.[21] In this modified basis the innermost core electrons (up to 3d) are described by the relativistic orbital-adjusted effective core potential of Hay and Wadt[22] and the remaining outer core and valence electrons by a [341/541/31] basis set where the two outermost 5p functions of the standard LANL2DZ basis set have been replaced by a [41] split of the 5p function optimized by Couty and Hall. For the Br atom[23] the quasi relativistic energy-adjusted spin-averaged effective core potential was taken from the work of the Stuttgart group, together with their [31/31] basis set, to which s and p diffuse functions (with exponents of 0.0493 and 0.0363, respectively) and a d polarization function (of exponent 0.381) were added, following Radom et al.[24] The car-

(15) For a few recent examples of tandem or cascade reactions that may involve Pd(IV) palladacycles, see for instance: (a) Catallani, M.; Frignani, F.; Rangoni, A. *Angew. Chem., Int. Ed. Engl.* **1997**, *36*, 119. (b) Catellani, M.; *Pure Appl. Chem*. **2002**, *74*, 63. (c) Ref 6. (d) Motti, E.; Mignozzi, A.; Catellani, M. *J. Am. Chem. Soc*. **2004**, *126*, 78. (e) Motti, E.; Rossetti, M. Bocelli, G.; Catellani, M. *J. Organomet. Chem*. **2004**, *689*, 3741. (f) Grigg, R.; Loganathan, V.; Stevenson, P.; Sukirthalingam, S.; Worakun, T. *Tetrahedron* **1996**, *52*, 11479. (g) Dyker, G. *Angew. Chem., Int. Ed. Engl.* **1992**, *31*, 1023. (h) Dyker, G. *Angew. Chem., Int. Ed. Engl.* **1994**, *33*, 103. (i) Dyker, G. *Angew. Chem., Int. Ed.* **1999**, *38*, 1699. (j) Albrecht, K.; Reiser, O.; Weber, M.; Knieriem, B.; de Meijere, A. *Tetrahedron* **1994**, *50*, 383. (k) de Meijere, A.; Meyer, F. E. *Angew. Chem., Int. Ed. Engl.* **1994**, *33*, 2379. (l) Huang, Q.; Campo, M. A., Yao, T.; Tian, Q.; Larock, R. C. *J. Org. Chem*. **2004**, *69*, 8251.

(16) Mota, A. J.; Dedieu, A.; Bour, C.; Suffert, J. *J. Am. Chem. Soc.* **2005**, *127*, 7171.

(17) Becke, A. D. *Phys. Rev. A* **1988**, *38*, 3098.

(18) Lee, C.; Yang, W.; Parr, R. G. *Phys. Rev. B* **1988**, *37*, 785.

(19) Becke, A. D. *J. Chem. Phys.* **1993**, *98*, 5648.

(20) Frisch, M. J.; et al. *Gaussian 03*, Revision B.04; Gaussian, Inc.: Pittsburgh, PA, 2003.

(21) Couty, M.; Hall, M. B. *J. Comput. Chem*. **1996**, *17*, 1359.

(22) Hay, P. J. *J. Chem. Phys.* **1985**, *82*, 299.

(23) Bergner, A.; Dolg, M.; Küchle, W.; Stoll, H.; Preuss, H. *Mol. Phys.* **1993**, *80*, 1431.

(24) Glukhovtsev, M.; Pross, A.; McGrath, M. P.; Radom, L. *J. Chem. Phys.* **1995**, *103*, 1878.

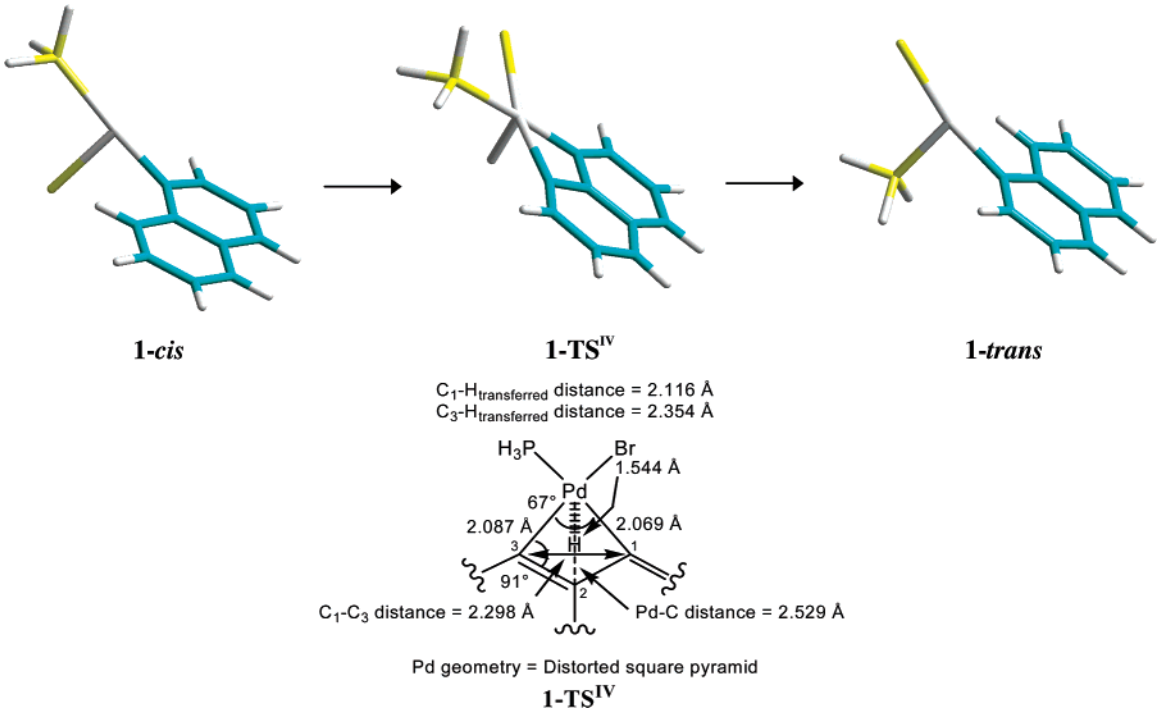

Figure 1. Optimized structures of the *cis* → *trans* Pd(IV) pathway for the 1,3 Pd migration in system **1**.

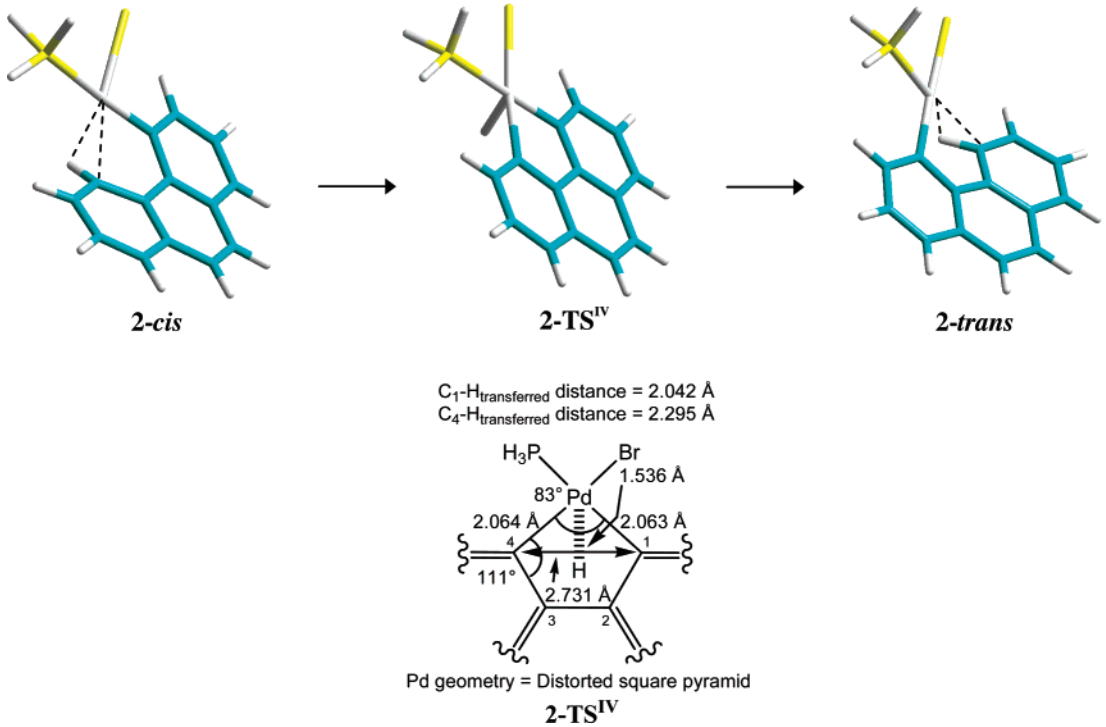

Figure 2. Optimized structures of the *cis* → *trans* Pd(IV) pathway for the 1,4 Pd migration in system **2**.

bon, hydrogen, and phosphorus atoms were described by the standard polarized 6-31G* basis set.[25,26] The nature of the optimized structures, either transition states or intermediates, was assessed through a frequency calculation. In some instances (see the Discussion section) we checked via an intrinsic reaction coordinate calculation that the computed transition state was indeed connecting the intermediates of interest. Since we are dealing here with intramolecular processes, we will concentrate on enthalpy values that were obtained by taking into account zero-point energies and the thermal motion at standard conditions (temperature of 298.15 K, pressure of 1 atm). We checked in our previous study[16] that the geometrical parameters obtained with this basis set are in agreement with related experimental structures of bromo-palladium complexes and that the thermodynamic values obtained with this basis set were quite comparable to those obtained with larger basis sets.[27−29]

(25) Hehre, W. J.; Ditchfield, R.; Pople, J. A. *J. Chem. Phys.* **1972**, *56*, 2257.
(26) Hariharan, P. C.; Pople, J. A. *Chem. Phys. Lett.* **1972**, *16*, 217.
(27) Alcazar-Roman, L. M.; Hartwig, J. F.; Rheingold, A. L.; Liable-Sands, L. M.; Guzei, I. A. *J. Am. Chem. Soc.* **2000**, *122*, 4618.
(28) Yin, J.; Buchwald, S. L. *J. Am. Chem. Soc.* **2002**, *124*, 6043.

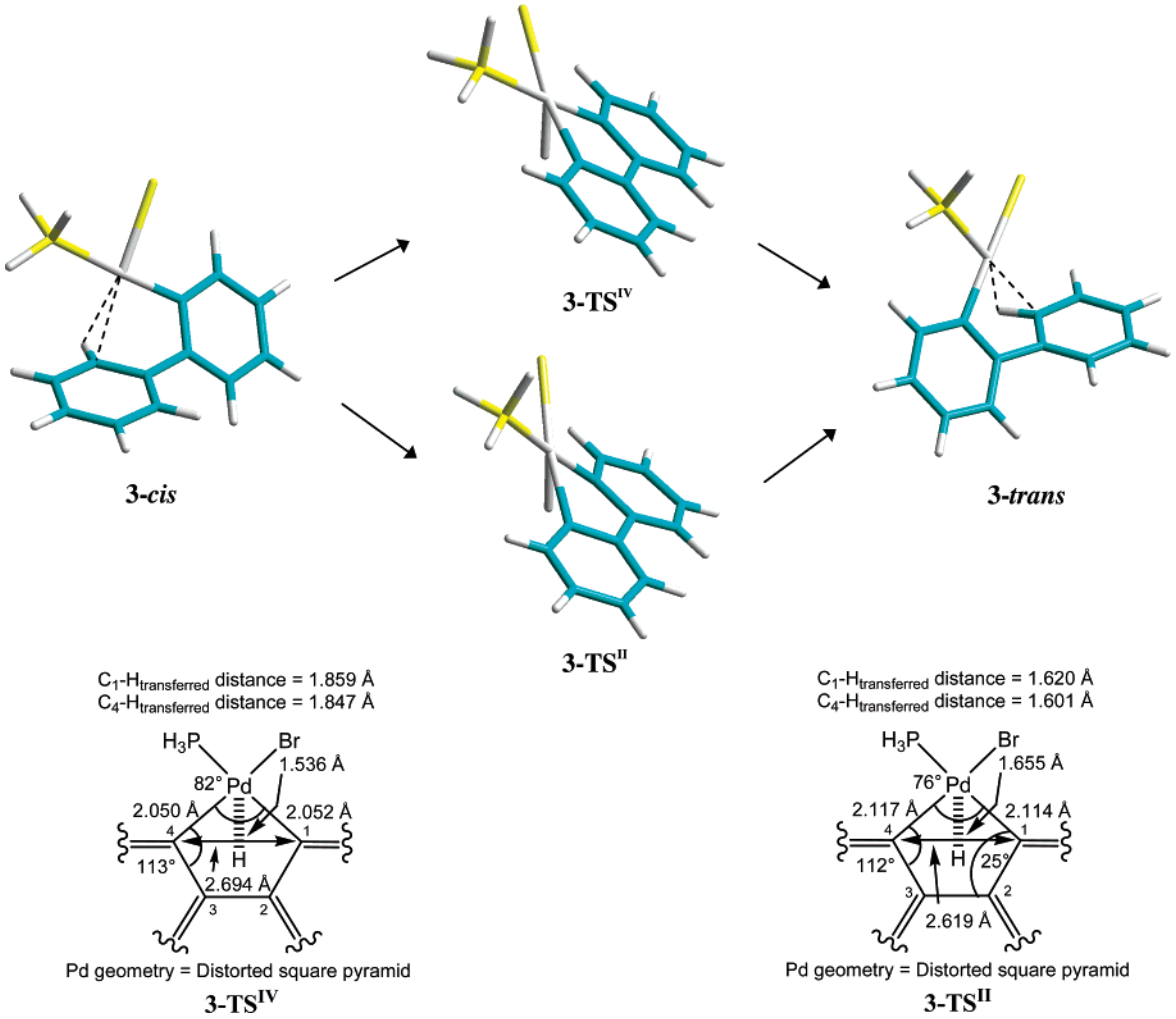

Figure 3. Optimized structures of the *cis* → *trans* Pd(II) and Pd(IV) pathways for the 1,4 Pd migration in system **3**.

Table 1. Energies (Δ*E*) and Enthalpies (Δ*H*) of the Transition States and Final Products for the *cis* → *trans* Transformation in Structures 1−3[a,b]

system		Δ*E*	Δ*H*	imaginary frequency[c]
1 (1,3 Pd migration)	**1-TS^{IV}**	+50.2	+46.6	335i
	1-*trans*	−6.4	−5.8	
2 (1,4 Pd migration)	**2-TS^{IV}**	+27.4	+24.4	379i
	2-*trans*	−4.6	−4.2	
3 (1,4 Pd migration)	**3-TS^{IV}**	+30.8	+27.5	409i
	3-TS^{II}	+32.5	+29.0	1372i
	3-*trans*	−4.9	−4.5	

[a] The values are in kcal mol^{-1}; the zero of energy for the Pd migration in **1**, **2**, and **3** refers to **1-*cis***, **2-*cis***, and **3-*cis***, respectively. [b] The B3LYP total energies (in au) are for **1-*cis***: $E = -868.590690$, $H = -868.410672$; for **2-*cis***: $E = -1022.237213$, $H = -1022.007957$; and for **3-*cis***: $E = -946.012679$, $H = -945.796471$. [c] In cm^{-1}, refers to the unique negative frequency of the calculated transition state.

Table 2. Energies (Δ*E*) and Enthalpies (Δ*H*) of the Transition States and Final Products Found for the *cis* → *trans* Transformation in Structures 4 and 5[a,b]

system		Δ*E*	Δ*H*	imaginary frequency[c]
4 (1,5 Pd migration)	**4-TS^{II}**	+21.0	+17.8	1392i
	4-*trans*	−4.7	−4.4	
5 (1,5 Pd migration)	**5-TS^{II}**	+26.8	+23.3	1281i
	5-TS1^{IV}	+39.4	+36.2	488*i*
	5-int^{IV}	+38.6	+36.0	
	5-TS2^{IV}	+39.4	+36.0	461i
	5-*trans*	−3.6	−3.3	

[a] The values are in kcal mol^{-1}; the zero of energy for the Pd migration in **4** and **5** corresponds to **4-*cis*** and **5-*cis***, respectively. [b] The B3LYP total energies (in au) are for **4-*cis***: $E = -1175.878351$, $H = -1175.599253$; and for **5-*cis***: $E = -985.327960$, $H = -985.081661$. [c] In cm^{-1}, refers to the unique negative frequency of the calculated transition state.

Results

The systems under investigation are the monopalladated polycyclic aromatic hydrocarbons (PAHs) **1**−**7**, the rearrangement of which is depicted in Scheme 2. As sketched in Scheme 3, these systems should result from an initial oxidative addition to palladium, of the carbon−bromine bond of the corresponding monobromated derivatives. Note that the *cis*/*trans* label here refers to the relative position of the bromine atom and the carbon atom covalently bound to palladium. For the product of this oxidative addition various structures can be anticipated depending on the coordination sphere around the palladium atom, and in particular on the number of phosphine ligands. Yet, a monophosphine Pd(II) bromo complex, formally three-coordinated, but that can display an additional relatively strong interaction between Pd and a pendant aryl ring, appears from our previous study to be an energetically favorable intermediate.[16] This is also in line with several experimental data.[27−36]

(29) Stambuli, J. P.; Incarvito, C. D.; Bühl, M.; Hartwig, J. F. *J. Am. Chem. Soc.* **2004**, *126*, 1184.

(30) Hartwig, J. F.; Paul, F. *J. Am. Chem. Soc.* **1995**, *117*, 5373.

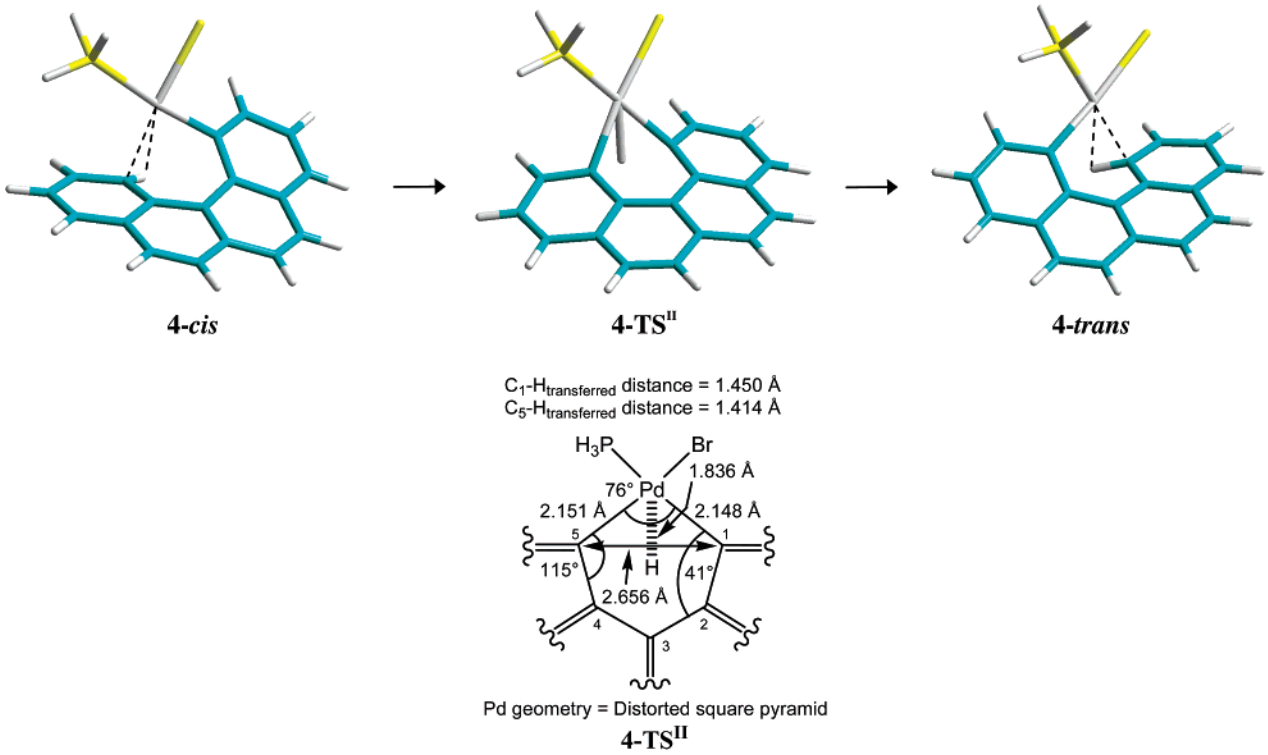

Figure 4. Optimized structures of the *cis* → *trans* Pd(II) pathway for the 1,5 Pd migration in system **4**.

Table 3. Energies (Δ*E*) and Enthalpies (Δ*H*) of the Transition States and Final Products Found for the *cis* → *trans* Transformation in Structures 6 and 7[a,b]

system		Δ*E*	Δ*H*	imaginary frequency[c]
6a (1,6 Pd migration)	**6a-TS^{II}**	+28.0	+24.3	1201i
	6a-TS1^{IV}	+42.4	+39.0	226i
	6a-int^{IV}	+42.3	+39.7	
	6a-TS2^{IV}	+45.4	+41.8	582i
	6a-*trans*	+1.2	+1.4	
6b[d] (1,6 Pd migration)	**6b-TS^{II}**	+23.1	+19.5	1165i
	6a-TS1^{IV}	+37.7	+34.3	226i
	6a-int^{IV}	+37.6	+35.0	
	6a-TS2^{IV}	+40.7	+37.8	582i
	6b-*trans*	−9.5	−8.9	
7 (1,6 Pd migration)	**7-TS^{II}**	+22.8	+19.3	1160i
	7-TS1^{IV}	+40.7	+37.2	616i
	7-int^{IV}	+38.4	+35.7	
	7-TS2^{IV}	+41.0	+37.4	604i
	7-*trans*	−4.1	−3.7	

[a] The values are in kcal mol^{-1}; the zero of energy for the Pd migration in **6a**, **6b**, and **7** corresponds to **6a-*cis***, **6b-*cis***, and **7-*cis***, respectively. [b] The B3LYP total energies (in au) are for **6a-*cis***: $E = -1024.637634$, $H = -1024.361180$; for **6b-*cis***: $E = -1024.630033$, $H = -1024.353675$; for **7-*cis***: $E = -1023.413247$, $H = -1023.160958$. [c] In cm^{-1}, refers to the unique negative frequency of the calculated transition state. [d] The Pd(IV) mechanism for **6b** follows the **6a** pathway.

Since the *cis*/*trans* enthalpy differences found throughout this study have been shown to be small (between 2 and 6 kcal mol^{-1}), the Pd/H rearrangement could be considered either in the *cis* → *trans* or in the *trans* → *cis* direction. Thus, it does not actually matter which initial isomer is formed in the early oxidative addition. Nevertheless, for reasons of coherence the Pd migration has been always considered from the *cis* isomer to the thermodynamically more stable *trans* isomer.[37]

Scheme 4. Geometric Features for 2-TS^{IV} and 3-TS^{II} Transition States

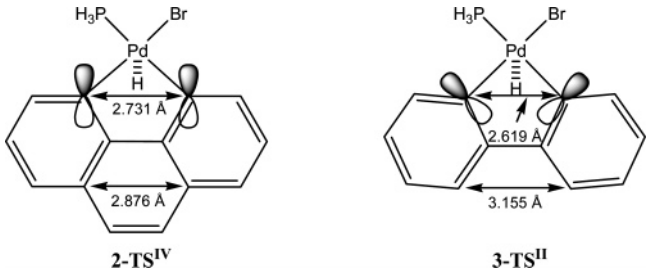

On going from **1** to **7**, see the Scheme 2, two structural series can be considered. First, beginning with **1** (1,3 Pd migration), we can successively add one and two phenyl rings to afford **2** (1,4 Pd migration) and **4** (1,5 Pd migration). Second, from the biphenyl system **3** (1,4 Pd migration), we can successively add one and two methylene groups between the two phenyl units to give the systems **5** (1,5 Pd migration) and **6** (1,6 Pd migration). In **7** (1,6 Pd migration) the ethyl bridge of system **6** has been replaced by an ethenic bridge. We will finally consider the transfer in the ethylene-vinyl complex **8**. In this system the Pd/H rearrangement can be viewed as being a 1 → ∞ transfer; see the Discussion section.

(A) 1,3 Pd Migration: Naphthalene System (1). One should first note that for this system the **1-*cis*** and **1-*trans*** isomers shown in Figure 1 display a genuine three-coordinated geometry due to the impossibility for the Pd atom to satisfy the fourth valence intramolecularly. In the other systems of Scheme 2 this

(31) Stambuli, J. P.; Bühl, M.; Hartwig, J. F. *J. Am. Chem. Soc.* **2002**, *124*, 9346.
(32) Galardon, E.; Ramdeehul, S.; Brown, J. M.; Cowley, A.; Hii, K. K.; Jutand, A. *Angew. Chem. Int. Ed.* **2002**, *41*, 1760.
(33) Paul, F.; Patt, J.; Hartwig, J. F. *J. Am. Chem. Soc.* **1994**, *116*, 5969.
(34) Louie, J.; Hartwig, J. F. *J. Am. Chem. Soc.* **1995**, *117*, 11598.
(35) Strieter, E. R.; Blackmond, D. G.; Buchwald, S. L. *J. Am. Chem. Soc.* **2003**, *125*, 13978.
(36) Hills, I. D.; Fu, G. C. *J. Am. Chem. Soc.* **2004**, *126*, 13178.

(37) Note that whereas a *trans*−*trans* rearrangement can take place and is found to be more energy demanding than the *cis*−*trans* rearrangement, a *cis*−*cis* rearrangement is not possible; see the Supporting Information for the corresponding analysis.

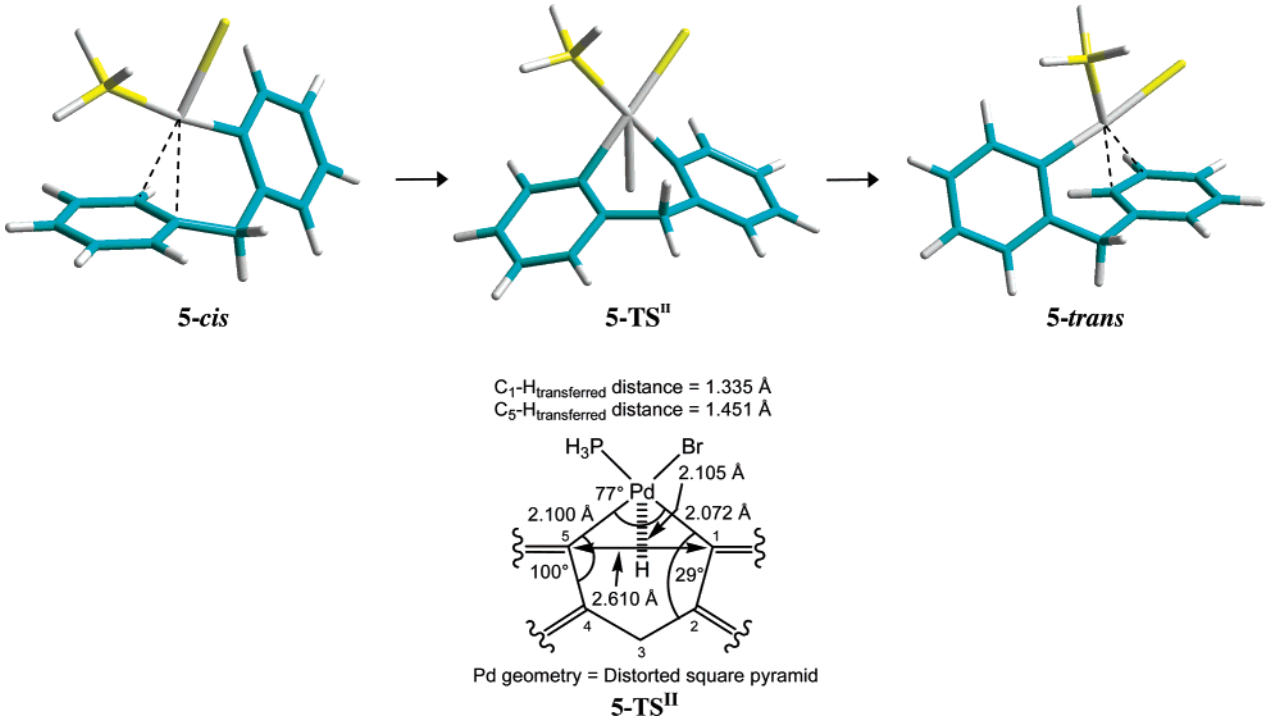

Figure 5. Optimized structures of the *cis* → *trans* Pd(II) pathway for the 1,5 Pd migration in system **5**.

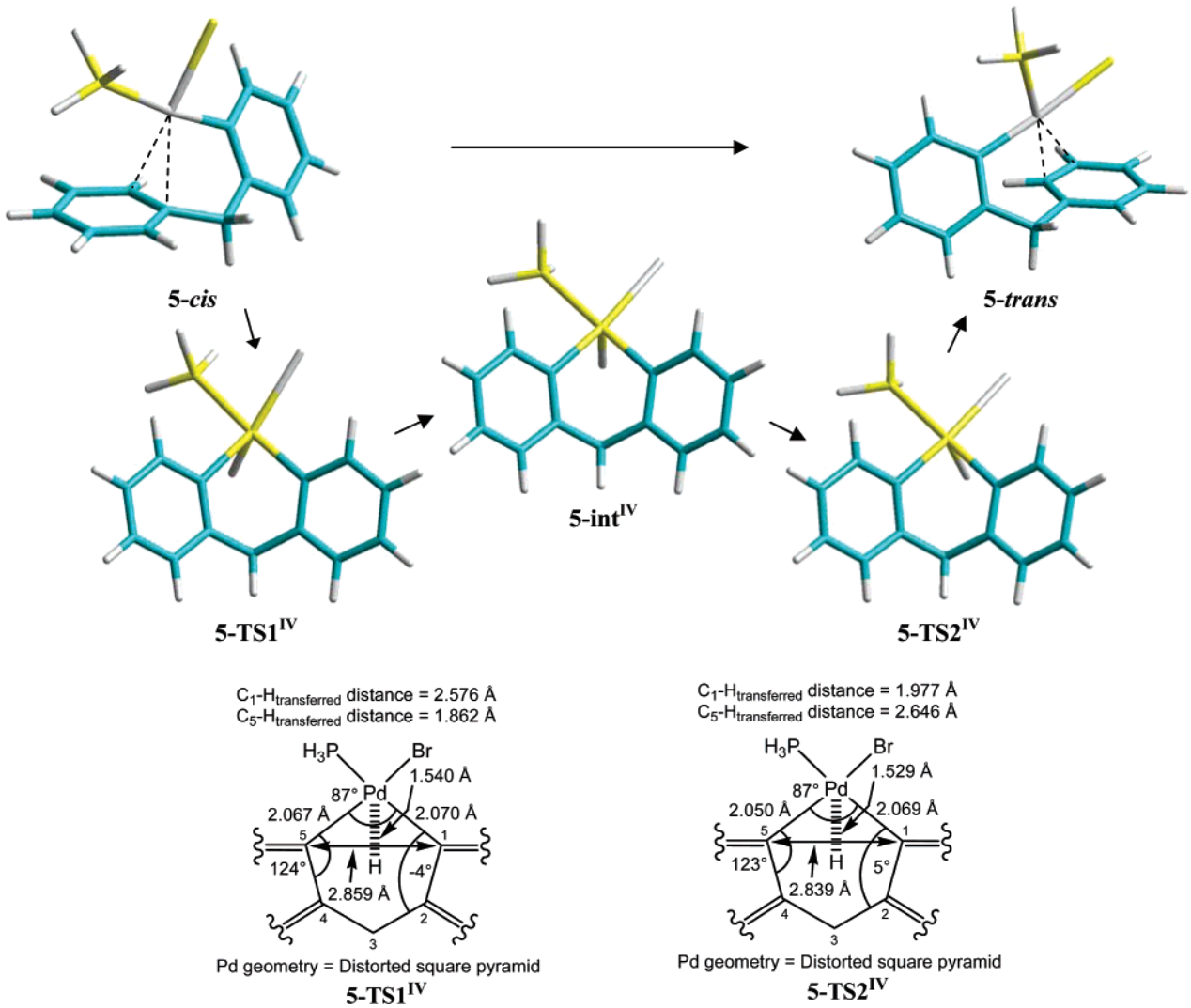

Figure 6. Optimized structures of the *cis* → *trans* Pd(IV) pathway for the 1,5 Pd migration in system **5**.

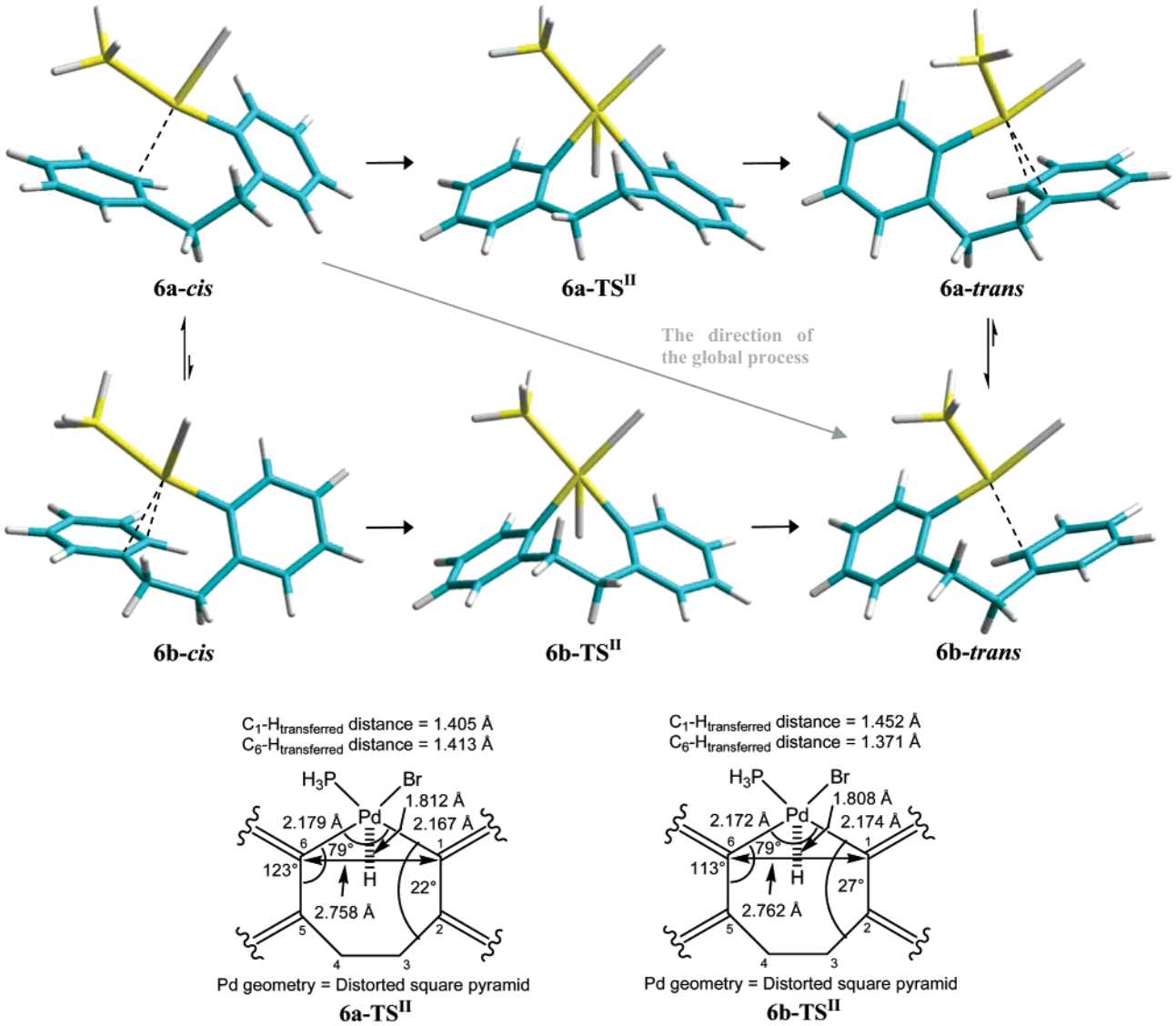

Figure 7. Optimized structures of the *cis* → *trans* Pd(II) pathway for the 1,6 Pd migration in system **6** (for conformers **a** and **b**).

valence is usually fulfilled by agostic interactions with a C−H bond of the neighboring aromatic unit.[16]

As far as the 1,3 intramolecular rearrangement is concerned, we found only one transition state, which, from an intrinsic reaction coordinate (IRC) calculation that we performed, clearly connects both the **1-*cis*** and **1-*trans*** structures in a single step.

Quite interestingly, however, is the fact that this transition state (**1-TS**^{IV}) is best viewed as being formally a d^6 Pd(IV) complex. This somewhat unexpected conclusion can be drawn from the consideration of the geometrical parameters: the Pd−$H_{transferred}$ distance is quite short, 1.544 Å, as found previously for the H transfer reaction through Pd(IV) intermediates.[16] In line with this feature, the distances between the transferred hydrogen atom and the two carbons involved in this transfer are rather long (2.12−2.35 Å), much longer than the distances that we computed for a genuine Pd(II) transition state.[16] Also of interest is the fact that in the **1-TS**^{IV} structure the Pd atom lies in the plane of the organic moiety (the Pd−C_1−C_2−C_3 dihedral angle amounting to 9°) and that the hydrogen atom, formally a hydride, is clearly at the apex of the H−Pd−Br−P plane, the corresponding dihedral angle amounting to 116°. We must stress here that a similar situation has been already encountered by Goddard and co-workers in their study of the mechanism of homogeneous Ir(III)-catalyzed arylation of olefins.[38] There, a d^4 Ir(V) transition state involving five covalent bonds was referred to as an "oxidative hydrogen migration" (so-called OHM) transition state. These authors subsequently found other OHM transition states implying a d^4 count for various transition metals.[39]

The activation energy for the 1,3 Pd transfer in system **1** is high (of the order of 50 kcal mol^{-1}; see Table 1). Hence this kind of process should be quite difficult. The main reason for this high activation barrier is the ring tension that the cyclometalated moiety experiences in the transition state, since the four-membered cycle results in a very small bite; see the C−Pd−C angle and C_1−C_3 distance in Figure 1.

(B) 1,4 Pd Migration: Phenanthrene (2) and Biphenyl (3) Systems. (B.1) Phenanthrene (2). In the case of the phenanthrene system (**2**), we also found a unique transition state (**2-TS**^{IV}, Figure 2) connecting the *cis* and *trans* isomers (as shown by an IRC calculation) through a direct Pd/H interchange. This transition state is again a formal Pd(IV) system, of OHM type,[38,39] with a structure akin to that of **1-TS**^{IV}: the Pd−$H_{transferred}$ distance amounts to 1.536 Å and the C−$H_{transferred}$

(38) Oxgaard, J.; Muller, R. P.; Goddard, W. A., III; Periana, R. A. *J. Am. Chem. Soc.* **2004**, *126*, 352.

(39) Oxgaard, J.; Periana, R. A.; Goddard, W. A., III. *J. Am. Chem. Soc.* **2004**, *126*, 11658.

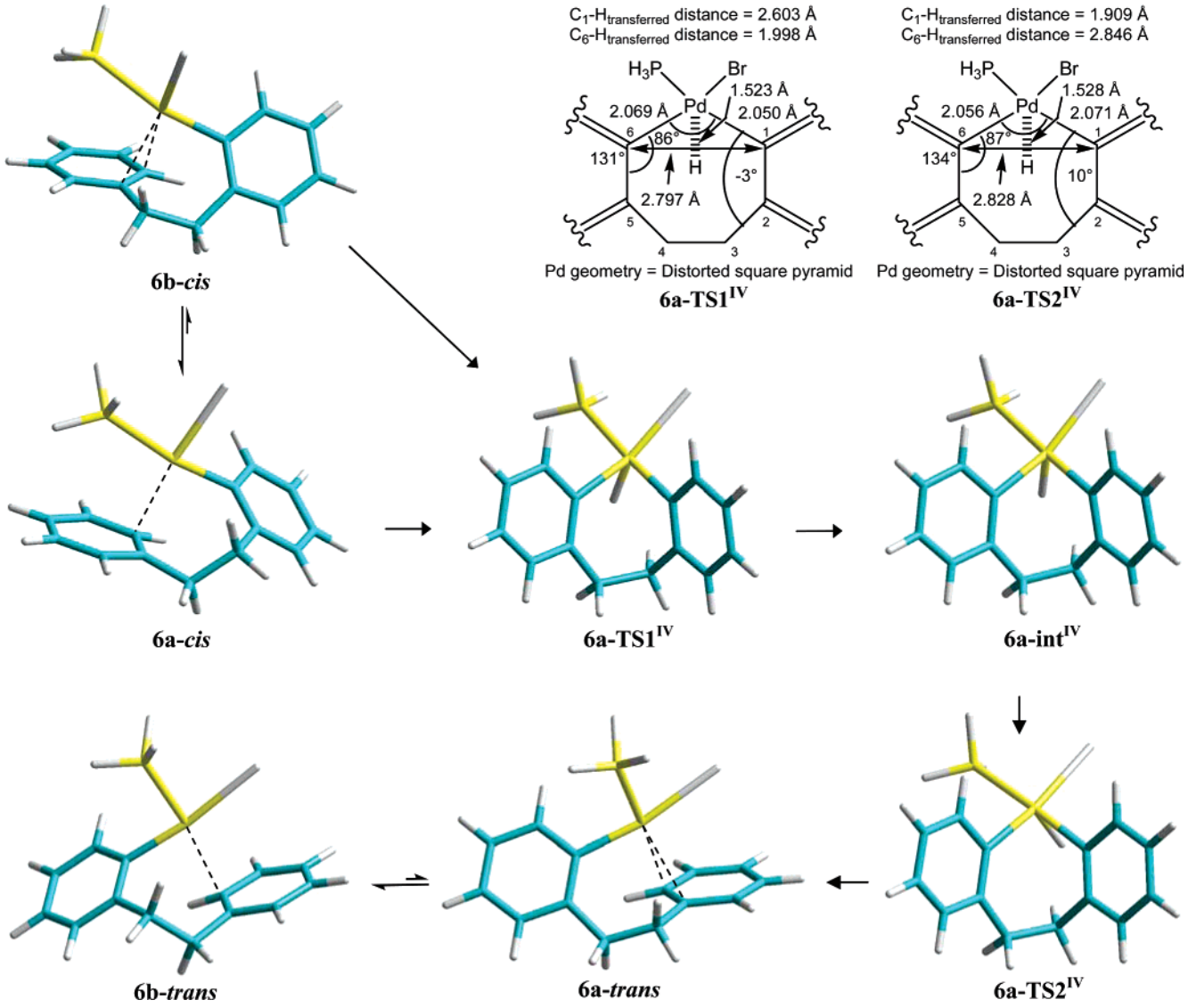

Figure 8. Optimized structures of the *cis* → *trans* Pd(IV) pathway for the 1,6 Pd migration in system **6** (for conformers **a** and **b**).

distances vary between 2.0 and 2.3 Å (Figure 2), i.e., similar values to those encountered for **1-TS^{IV}** (Figure 1).

That steric factors are strongly involved in the height of the energy barrier appears clearly from the comparison between **1** and **2**. **2-TS^{IV}** is geometrically much more relaxed than **1-TS^{IV}**, and the corresponding activation enthalpy drastically falls from +46.6 (**1-TS^{IV}**) to +24.4 kcal mol^{-1} (**2-TS^{IV}**) (Table 1).

(B.2) Biphenyl (3). In contrast to the previous systems, our calculations now point to *two* transition states that could operate for the *cis* → *trans* conversion; see Figure 3 (and Figure S1 of the Supporting Information for a side-view of these transition states). The first one is the Pd(IV) structure **3-TS^{IV}**, geometrically very similar to **1-TS^{IV}** and **2-TS^{IV}**. The only exception is the C−H$_{transferred}$ distances, which are shorter in **3-TS^{IV}** (in fact, one can observe a diminution of these distances on going from system **1** to **3**; see Figures 1−3). As for **1** and **2**, *this transition state corresponds to a single-step mechanism for the Pd/H interchange* (through a hydride transfer), with an activation barrier comparable to that found for phenanthrene (**2**) (see Table 1). Note also from Table 3, that—as in the Ir(V) system of Goddard and co-workers[38]—these OHM type transition states are characterized by a rather low imaginary frequency (between 300i cm^{-1} and 400i cm^{-1}), much lower than the one found in the Pd(II) transition states.

The second one, which also corresponds to a direct Pd/H interchange (**3-TS^{II}**, Figure 3), is best characterized, however, as involving a +2 oxidation state for the Pd atom. Its geometry is indeed quite similar to that reported in our previous work for a 1,5 Pd(II) migration and different from that obtained for **3-TS^{IV}** (compare for instance the C−H$_{transferred}$ and Pd−H$_{transferred}$ distances in Figure 3). Thus, in this case the single-step Pd/H rearrangement process corresponds formally to a proton transfer. Interestingly too, both Pd(II) and Pd(IV) transition states have very similar energies (the Pd(IV) pathway being only slightly favored), and therefore both mechanisms can be considered as being competitive (Table 1).

Comparing the 1,4 Pd migration in the biphenyl (**3**) and phenanthrene (**2**) systems, we noticed that **2** has a more rigid structure. Hence the occurrence of a Pd(II) transition state in **3**, and not in **2**, is most likely due to the possibility of slightly distorting the organic moiety: in **3-TS^{II}**, the two phenyl rings are somewhat tilted back toward Pd, as seen from the distances reported in Scheme 4. The flexibility of the organic moiety attached to the metallic center seems to be a determinant feature that allows for these Pd(II) transition states. In fact, the orientation of the organic moiety with respect to the hydrogen is rather different in both Pd(II) and Pd(IV) transition states, the former having orbitals oriented to the inner

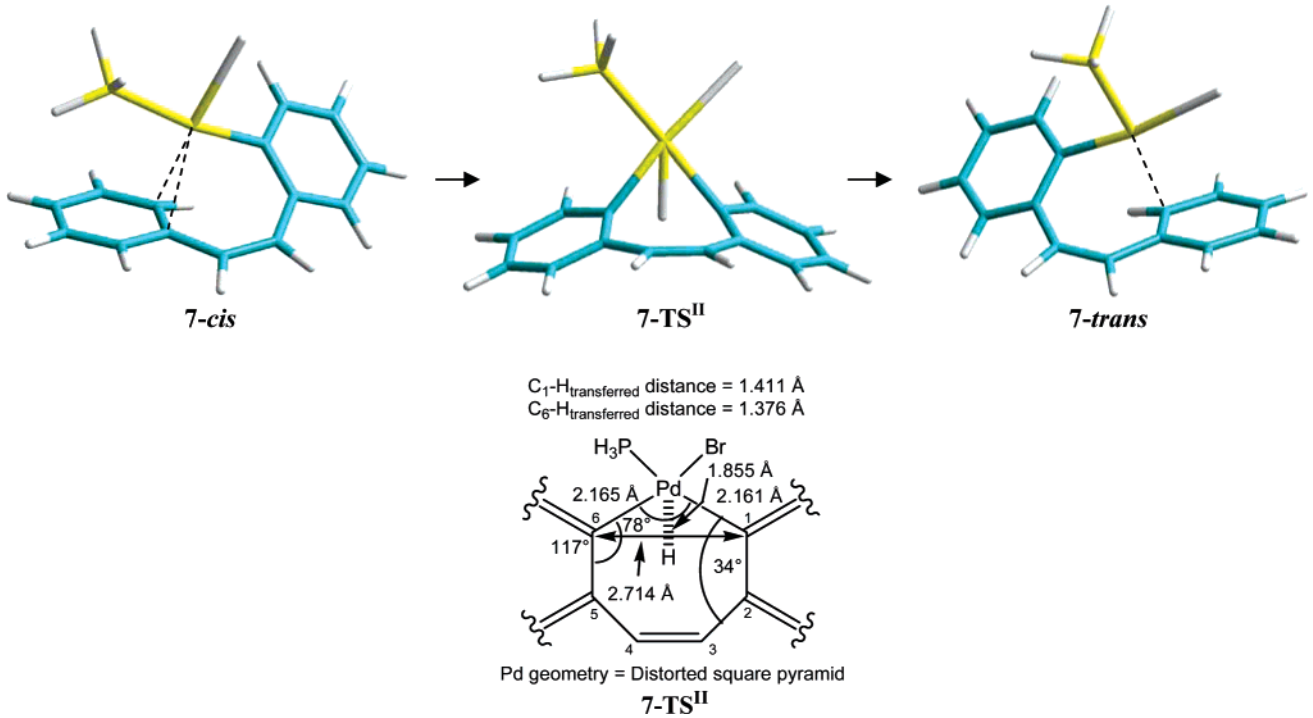

Figure 9. Optimized structures of the *cis* → *trans* Pd(II) pathway for the 1,6 Pd migration in system **7**.

C−Pd−C space in order to assist the transfer of the hydrogen (vide infra).

Scheme S1 summarizes the various energy profiles obtained for the *cis* → *trans* conversion in the systems **1**−**3**; see the Supporting Information.

(C) 1,5 Pd Migration: Benzo[*c*]phenanthrene (4) and Benzylbenzene (5) Systems. (C.1) Benzo[*c*]phenanthrene (4). The 1,5 aryl-to-aryl Pd migration in system **4** differs significantly from the migration in the systems **1**−**3**. The most salient feature is the absence of a Pd(IV) route connecting directly the *cis* and *trans* isomers. The only transition state that we could locate corresponds to a +2 oxidation state (**4-TS^{II}** in Figure 4). That a sp^2 → sp^2 1,5 Pd migration involves, for the single-step mechanism, a Pd(II) transition state rather than a Pd(IV) one is in agreement with our previous results obtained in the case of vinyl-to-aryl Pd migrations.[16] The geometry observed for **4-TS^{II}** is indeed very similar to that of the Pd(II) transition states calculated in these vinyl-to-aryl migrations[16] and quite different from the one obtained for the Pd(IV) transition states in **1**−**3**: the Pd−$H_{transferred}$ and C−Pd distances are longer, the C−$H_{transferred}$ distances are shorter, and the Pd atom is no longer in the plane of the organic moiety (25° in **3-TS^{II}** and 41° in **4-TS^{II}**). As far as the energetics is concerned, the **4-TS^{II}** transition state is quite low in energy (Table 2), in fact the lowest of all the calculated transition states throughout this study (vide infra).

(C.2) Benzylbenzene (5). As in **4**, we found a Pd(II) transition state (**5-TS^{II}**) for the single-step mechanism, akin to **4-TS^{II}** (Figure 5). The corresponding activation barrier (see Table 2) is, however, somewhat larger than the one calculated for system **4** and more comparable to that calculated for the Pd(II) pathway in **3**. Although one might trace this feature to an unfavorable steric component arising from the sp^3 (alkyl) fragment between the two cycles, we think that it is due to a better stabilization of the *cis* structure of **5** compared to **4**: the presence of the methylene group between both aromatic rings in **5** allows a more effective Pd-phenyl complexation with less strain energy, resulting in a *cis* complex that is well stabilized. Since these factors do not come into play in the corresponding transition states (see Figures 4 and 5), the outcome is a higher barrier for system **5** compared to that of system **4**. The same reasoning can be applied to the activation barrier difference found for the Pd(IV) mechanism in systems **2** and **3** (represented respectively by the transition states **2-TS^{IV}** and **3-TS^{IV}**; see Scheme S1).

We also found a Pd(IV) route for the *cis* → *trans* conversion process. However, in contrast to the previous cases studied (systems **1**−**3**), for which a single-step Pd(IV) pathway was obtained, *this route is now a two-step sequence* with a Pd(IV) intermediate between the oxidative addition step and the reductive elimination step. As seen in Figure 6, the optimized geometries for the intermediate and transition states are square pyramidal with the hydrogen atom in the apical position. The energy requirement for this Pd(IV) route, formally based on a hydride transfer, is quite high, 36.2 instead of 23.3 kcal mol^{-1} for the Pd(II) pathway (Table 2).

Scheme S2 summarizes the energy profiles for the possible mechanisms involved in the *cis* → *trans* conversion found in systems **4** and **5**; see the Supporting Information.

(D) 1,6 Pd Migration: Phenethylbenzene (6) and Styrylbenzene (7) Systems. (D.1) 1,6 Pd migration: Phenethylbenzene (6). Adding an additional methylene group to the alkyl chain binding the two phenyl groups results in the phenethylbenzene system **6**. The calculations carried out for the 1,6 Pd migration in this system point again to a relatively easy *cis* → *trans* conversion via a Pd(II) single-step process. Yet, there is some additional complexity due to the existence of two conformers (**6a** and **6b**) for each *cis* or *trans* isomer; see Figure 7. For the *cis* isomer, the **6a** conformer is more stable than **6b** by 4.7 kcal mol^{-1}, whereas for the *trans* isomer, the **6b** conformer is more stable than **6a** by 5.6 kcal mol^{-1} (enthalpy values). The energetics of the process is summarized in Table 3 and Scheme S3 (see the Supporting Information). Should there be a thermodynamic control for the *cis* → *trans* reaction, the **6a-*trans*** complex, once formed, would quantitatively evolve to the thermodynamically more stable **6b-*trans*** conformer. On

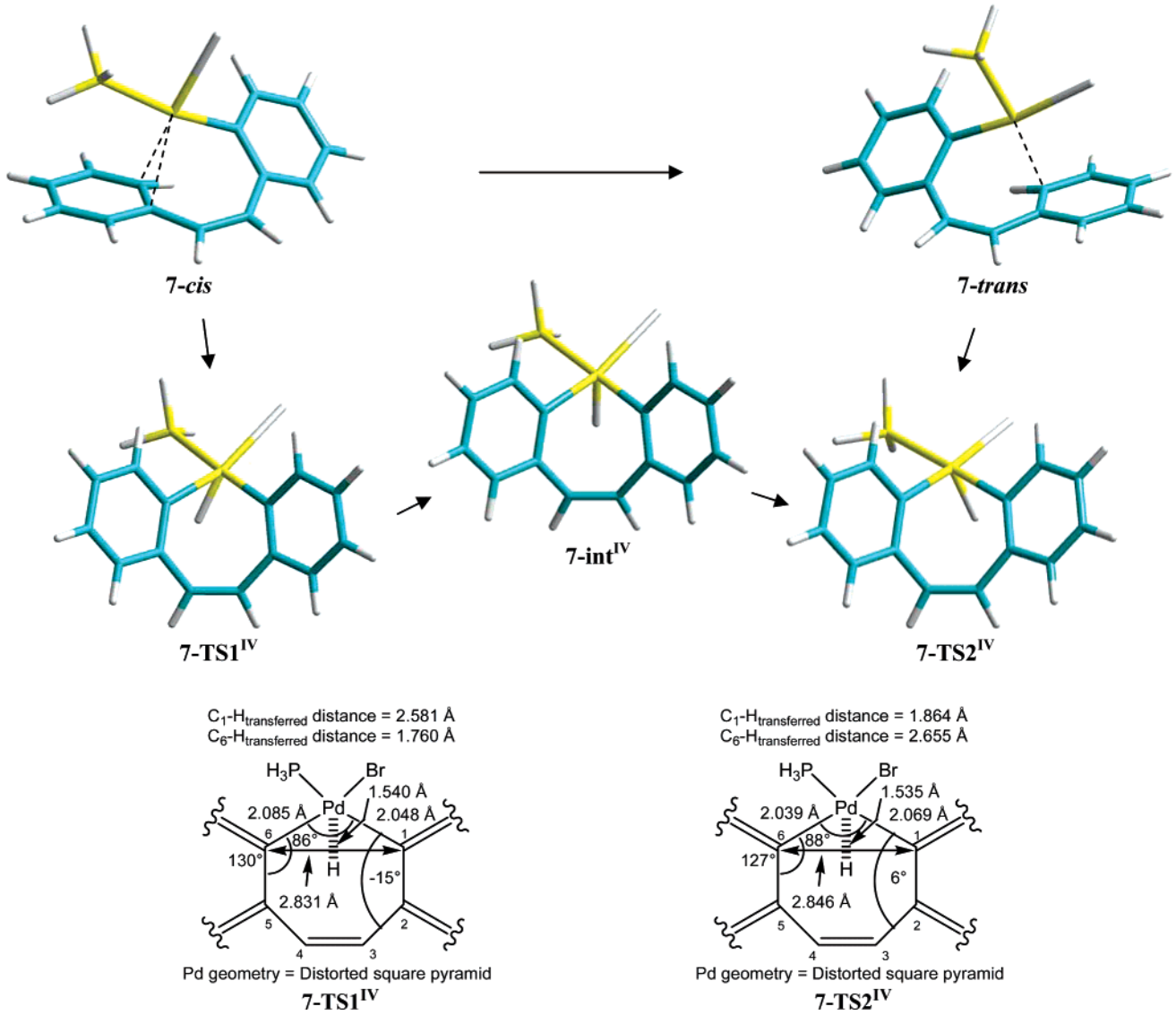

Figure 10. Optimized structures of the *cis* → *trans* Pd(IV) pathway for the 1,6 Pd migration in system **7**.

the other hand, should the reaction be kinetically controlled, then the conversion rate from **6b-*cis*** would be higher (estimation from the calculated activation barriers, Table 3), the system going again to the thermodynamically more stable **6b-*trans*** structure.

As in **5**, we found a two-step Pd(IV) pathway operating for the *cis* → *trans* conversion; see Figure 8. This pathway is energetically very unfavorable compared to the Pd(II) single-step process; see Table 3 and Scheme S3. Note that no Pd(IV) transition state originating from **6b** could be found, all optimization attempts invariably leading to the **6a-TS1^{IV}** structure.

(D.2) 1,6 Pd Migration: Stirylbenzene (7). The ethyl bridge of **6** was replaced by an ethenic bridge in **7**. This led to a decrease of about 5.0 kcal mol^{-1} for the calculated activation enthalpy of the Pd(II) pathway in **7** compared to **6** (see Table 3 and Scheme S3). The reason for this decrease is most probably a poorer stabilization of the **7-*cis*** isomer due to the introduction of a more rigid double bond, rather than the elimination of steric constraints in the transition state. Figure 9 shows this pathway for system **7** (note that in contrast to **6**, no conformational considerations have to be taken into account).

As in **6**, we also found a two-step Pd(IV) pathway connecting the *cis* and *trans* isomers (Figure 10), but the corresponding barrier is again much higher than the barrier for the Pd(II) pathway (see Table 3 and Scheme S3). Thus, for both systems that are prototypes for a 1,6 Pd migration (**6** and **7**), the *two-step* Pd(IV) *cis* → *trans* conversion seems to be very unlikely.

Discussion

To delineate the geometric and electronic factors that govern the preference for one pathway over the others, we thought that it would be interesting to consider a 1,*n* migration in which the connection between the two organic sides has been removed, viz., to consider a system with two disconnected organic molecules. This would in particular allow looking at the Pd/H interchange on an unconstrained system, both sides being able to adopt the more adequate position with respect to the palladium atom. We thus chose the ethylene molecule as the simplest model for the organic ligand from which a hydrogen atom is transferred to a vinyl−palladium bond; see Figure 11. The calculations led to two single-step transition states, formally of Pd(II) and Pd(IV) character. The corresponding structures and energies are displayed in Figure 11 and Table 4, respectively.

Looking first at the structural and electronic aspects, one may notice that in the Pd(II) transition state **8-TS^{II}** the transferred hydrogen is located precisely in the C−Pd−C plane. In fact,

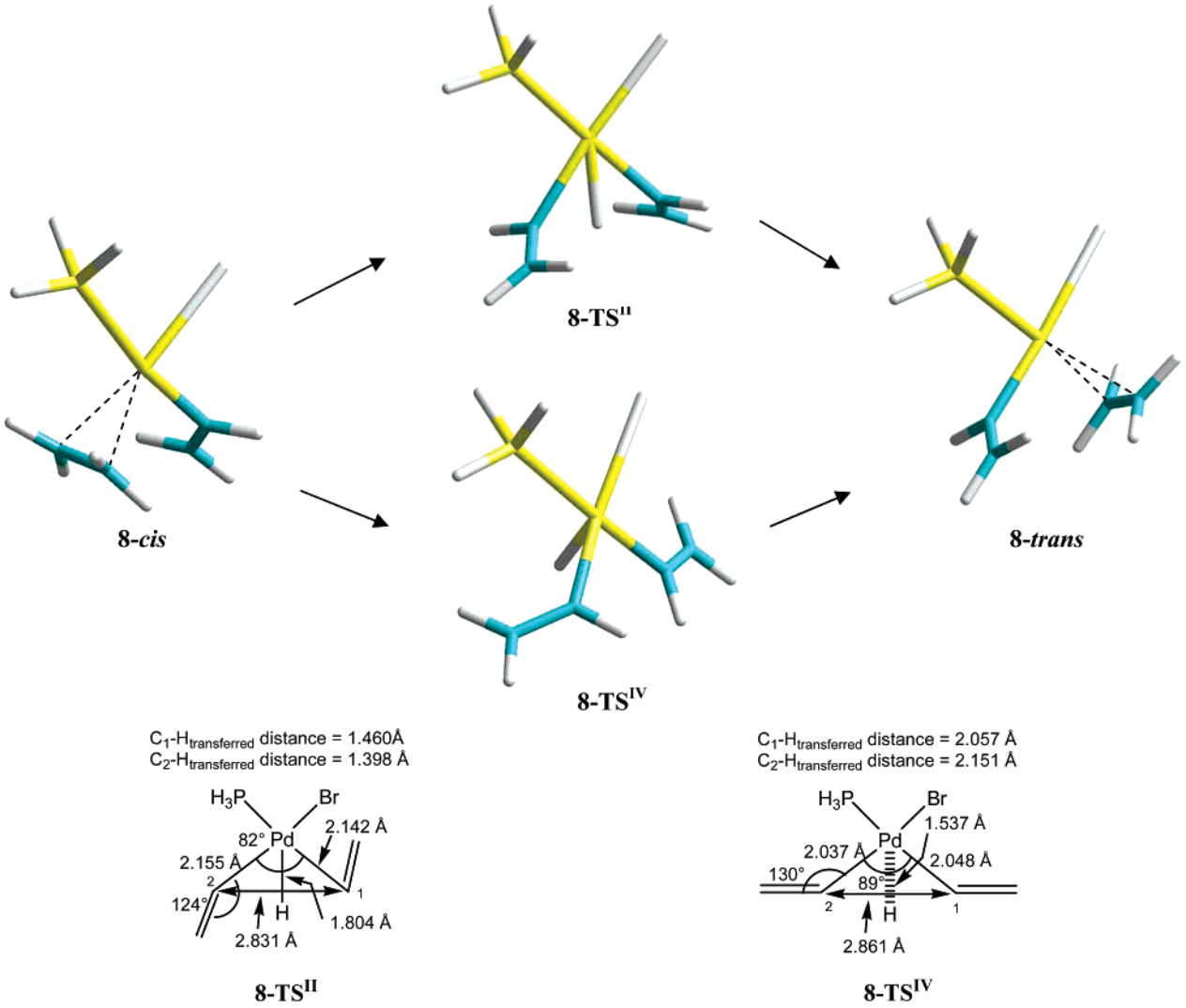

Figure 11. Optimized structures of the *cis* → *trans* Pd(II) pathway for the 1,∞ Pd migration in system **8**.

Table 4. Energies (Δ*E*) and Enthalpies (Δ*H*) of the Transition States and Final Products Found for the *cis* → *trans* Transformation in Structure 8[a,b]

system		Δ*E*	Δ*H*	imaginary frequency[c]
8 (1,∞ Pd migration)	**8-TS^{IV}**	+47.7	+43.9	240i
	8-TS^{II}	+35.0	+31.4	1232i
	8-*trans*	−4.8	−4.4	

[a] The values are in kcal mol^{-1}; the zero of energy refers to **8-*cis***. [b] The B3LYP total energies (in au) are for **8-*cis***: $E = -639.914292$, $H = -639.776793$. [c] In cm^{-1}, refers to the unique negative frequency of the calculated transition state.

on going from the 1,4 to the 1,∞ rearrangement, one can observe a gradual change of the hydrogen from an out-of plane to an in-plane position. This is best illustrated by the variation of the H−Pd−Br−P improper torsion angle, which measures the displacement of the hydrogen atom from the plane defined by the metallic moiety; see Scheme 5: +145° in **3-TS^{II}**, +163° in **4-TS^{II}**, +170° in **6a-TS^{II}**, and +184° in **8-TS^{II}**. This angle also correlates with the C−Pd−C−C dihedral angle, which characterizes the displacement of the palladium atom with respect to the plane defined by the organic moiety; see Scheme 5: +30° in **3-TS^{II}**, +64° in **4-TS^{II}**, +77° in **6a-TS^{II}**, and +97° in **8-TS^{II}**. We can relate the variation of these angles to steric factors. In **3** the calculated distance between the two carbons involved in the Pd/H rearrangement is 2.619 Å, whereas it amounts to 2.831 Å in the model **8**. This implies that the transferred hydrogen atom is more hindered in **3** and must be placed out of the C−Pd−C plane. Note also that the two vinyl groups of the **8-TS^{II}** structure are not coplanar with the $PdBr(PH_3)$ unit (the Br−Pd−C−H and P−Pd−C−H dihedral angle amounting to 66° and 78°, respectively), but adopt a structure that is reminiscent of their structure in **8-*cis*** and **8-*trans*** (see Figure 11), so as to clamp the transferred hydrogen.

Scheme 5. Displacement of the Hydrogen Atom from the Plane Defined by the Metallic Moiety (left) and Displacement of the Palladium Atom with Respect to the Plane Defined by the Organic Moiety (right)

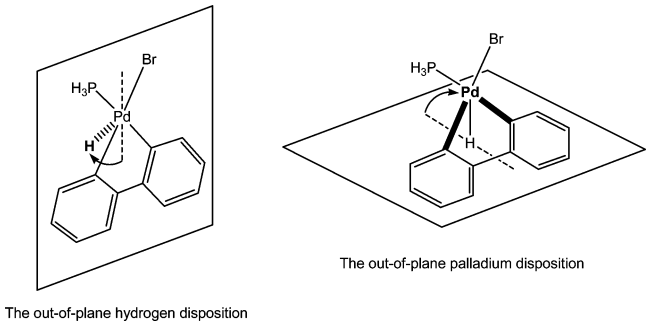

The results of the orbital analysis for **8-TS^{II}** are in line with the above features. The three occupied orbitals that have a

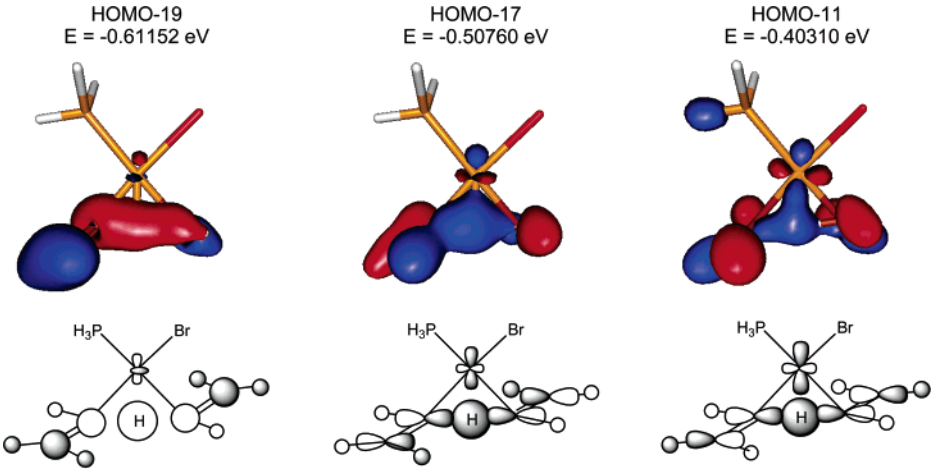

Figure 12. Orbitals contributing to the hydrogen transfer in Pd(II) transition states.

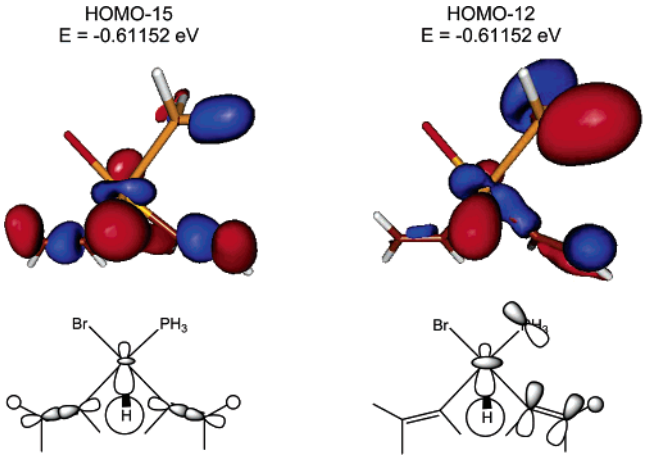

Figure 13. Orbitals contributing to the hydrogen transfer in Pd(IV) transition states.

significant weight on the transferred hydrogen all correspond to a bonding combination between the hydrogen s orbital and the occupied orbitals belonging to the σ framework of the two C_2H_3 fragments; see Figure 12. There is also some contribution from a nonbonding (with respect to the spectator ligands) d orbital on palladium. Thus the transfer does correspond to a through-space proton transfer between the two carbon atoms, somewhat assisted by the metal. As mentioned above, this proton transfer takes place in the PdC_2 plane. We have previously provided a rationalization of this feature on the basis of the isolobal analogy of such transition states with CH_5^+ in the C_s geometry.[16] At this stage it is important to underline that the formal oxidation state of +2 for **8-TS^{II}** is well reflected in the nature of its lowest unoccupied molecular orbital (LUMO), which is—as expected in a square planar Pd(II) complex—the $d_{x^2-y^2}$ orbital (somewhat antibonding with the ligands' σ orbitals), the d_{z^2} orbital being one of the four doubly occupied metal d orbitals.

The Pd(IV) transition state, on the other hand, has the transferred hydrogen atom placed almost apically with respect to the plane defined by the ligands of the metal. Note also that the two C_2H_3 groups are now more coplanar with the PdBr(PH_3) group; see Figure 11. We found two occupied orbitals with a significant weight on the transferred hydrogen, Figure 13. They both involve a bonding combination of the s orbital of the transferred hydrogen with the palladium d_{z^2} type orbital. The LUMO of the system is made of the corresponding antibonding combination between d_{z^2} and s_H, and the next LUMO is the antibonding combination of $d_{x^2-y^2}$ with the ligand σ orbitals. Thus, the system has an electronic structure that indeed corresponds to that of a square pyramid d^6 complex (i.e., a Pd(IV) complex), the transferred hydrogen being formally a hydride.

As far as the activation energies are concerned, one should first note that, for a system like **8**, which is devoid of any geometrical or steric constraints, the Pd(II) pathway is favored over the Pd(IV) pathway by about 12 kcal mol^{-1} (ΔH values). This is consistent with the known difficulty of palladium complexes to achieve a +4 oxidation state. Yet the energy demand is quite high in both pathways. We trace this feature again to a relatively strong stabilization of the **8-*cis*** species, for which there is no spatial restrictions to accommodate simultaneously the ethylene and the vinyl ligands.

In fact in all the transfers that we have investigated so far, the geometric factors that are induced by the electronic requirements play an important role in the transition states as in the reactants. We have underlined above that a Pd(II) transition state is helped by a clamping arrangement of the two organic moieties, in contrast to the Pd(IV) transition state, for which a planar arrangement is more favorable. Thus **1** and **2**, which cannot achieve this clamping arrangement, are characterized by the existence of a Pd(IV) transition state only, whereas for **3**, **4**, **5**, **6**, and **7** both Pd(II) and Pd(IV) transition states can be located. The ease of the Pd(II) pathway in these systems will result from the balance between the propensity of the two organic moieties to achieve this clamping arrangement and the ability of the metallic fragment to fill the fourth coordination intramolecularly either via an agostic interaction with a C−H bond (systems **3** and **4**) or via a π interaction with a C−C bond (systems **5**, **6**, and **7**). The Pd(IV) transition states are generally much higher in energy, as expected for this +4 oxidation state, the only exceptions being **2** and **3**. This is due to the fact that in these systems the coplanar arrangement of the two organic moieties in the transition state is easily achieved, the ring tension in the metallacycle is not too large (contrary to **1**), and the reactant is not stabilized too much since it experiences only a C−H agostic interaction, which is relatively weak.

We finally note that the Pd(IV) route can take place in either one or two steps. It is clear from the analysis of the 1,4 to 1,6 transfer that the preference for the one-step pathway over the two-step pathway has its origin in structural requirements. A single-step Pd(IV) transfer will take place when the transferred hydrogen has the possibility to interact simultaneously with both

Scheme 6

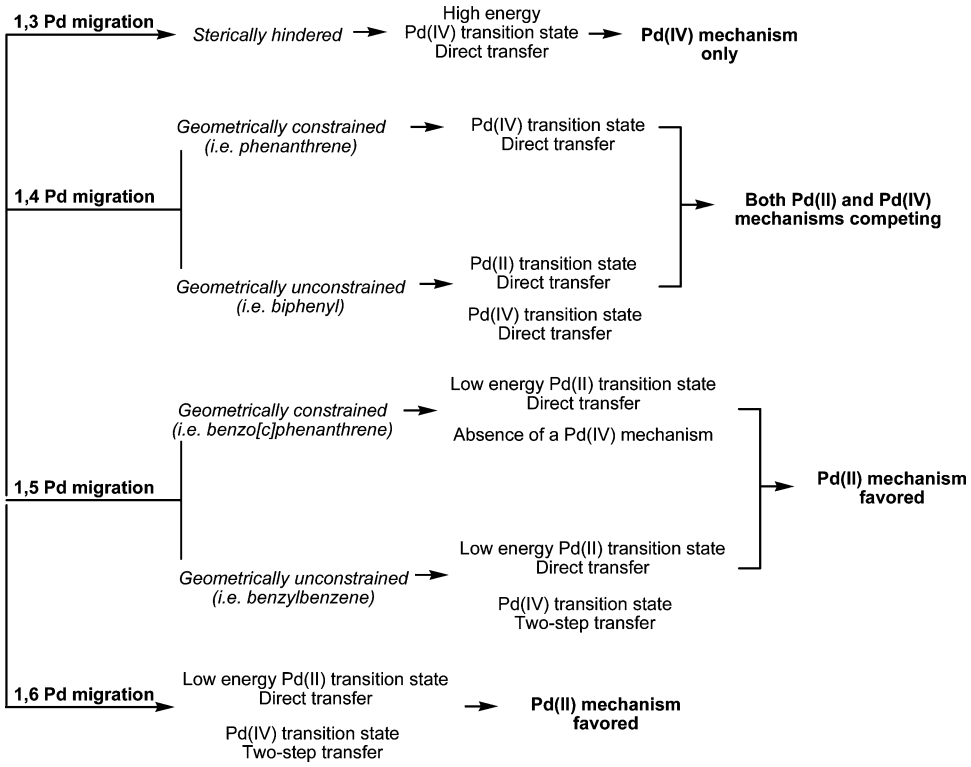

organic sides. Conversely, if the system cannot set up such a structure, due to geometric requirements (as in systems **5**, **6**, and **7**), one finds an intermediate connected by two transition states in which the hydrogen atom interacts more with the carbon atom to which it will be transferred than with the other.

All the above conclusions can be summarized in Scheme 6.

Conclusion

We have investigated through this study, based on DFT-B3LYP calculations, the possible mechanism operating for intramolecular 1,*n* aryl-to-aryl palladium shifts (which are simultaneously accompanied by a hydrogen migration). From our calculations, the active species in the *cis* → *trans* conversion process appear to be distorted square pyramidal Pd(IV) and/or Pd(II) forms. The Pd(IV) route (formally involving a hydride transfer in an oxidative hydrogen migration mechanism) is the preferred mechanism for 1,3 Pd migrations, whereas the Pd(II) pathway (formally involving a proton transfer) turns out to be much more favorable in the case of 1,5 and 1,6 Pd migrations. In the case of 1,4 Pd/H interchanges, however, both mechanisms become competitive, displaying similar activation energies. This has been rationalized in terms of geometric factors, namely, the ability of the two organic moieties either to adopt a clamping arrangement with respect to the transferred hydrogen in the Pd(II) transition state or to be roughly coplanar in the Pd(IV) transition state. The orbital analysis that we have performed on the $PdBr(PH_3)(C_2H_3)(C_2H_4)$ model system does support these conclusions. We are now extending our investigations to alkyl → aromatic Pd migrations.

Acknowledgment. The calculations have been carried out on the workstations of our laboratory, of the Centre Universitaire Régional de Ressources Informatiques (CURRI) of Strasbourg, and of the Institut du Développement et des Ressources en Informatique Scientifique (IDRIS, Orsay). We thank Dr. L. Padel and Mrs. S. Fersing for their technical assistance. A.M. gratefully acknowledges the Spanish government (Junta de Andalucía−Universidad de Granada) for the financing of his postdoctoral stay in Strasbourg.

Supporting Information Available: Side-view of **3-TS^{II}** and **3-TS^{IV}** transition states, energy profiles for systems **1**−**7**, *trans* → *trans′* transformations for systems **3**−**7**, and 1,4 versus 1,5 Pd migration in systems **9** and **10**. This material is available free of charge via the Internet at http://pubs.acs.org. Cartesian coordinates for all the calculated structures are available, on request, from the corresponding author.

OM060128A